vanadium and chromium. A "soft" contribution to the interaction energy may be schematically introduced according to

$$\Delta A = \Delta A_{\text{Coulomb}} + \Delta A_{\text{soft}} \tag{8}$$

The softer the metal ion, the stronger its covalent interaction with thiocyanate, and thus an increasing *positive* contribution, ΔA_{soft}, to the total interaction energy would be the result. Hence, the effect of introducing ΔA_{soft} is to counteract the ligand exchange (1) to various extents for the acceptor ions considered here. Ahrland[26] suggested that a softness parameter, basically the sum of ionization energy and hydration enthalpy, may be taken as a good measure of the softness character of acceptor ions. This approach was later elaborated by Marcus,[27] who demonstrated the applicability of the softness scale to molten salt mixtures. The softness character decreases in the orders $Cr^{3+} > V^{3+} \approx Al^{3+}$ and $SCN^- > F^-$. ΔA_{soft} is thus expected to increase in the order $Cr^{3+} > V^{3+} \approx Al^{3+}$, which may be the underlying reason for the interchange of chromium(III) and vanadium(III) in the observed stability sequence as compared to the one calculated from a hard-sphere model. The predictive power of the schematic eq 8 might be explored in a more quantitative aspect by correlating a larger amount of experimental thermodynamic data on complexation in melts with ionic charges, interatomic distances, and softness parameters.

Acknowledgment. We thank Dr. Börje Folkesson, who performed the ESCA analysis. This work has also been supported by the Swedish Natural Science Research Council.

Supplementary Material Available: A listing of experimental emf data (4 pages). Ordering information is given on any current masthead page.

---

(26) Ahrland, S. *Chem. Phys. Lett.* **1968**, *2*, 303.
(27) Marcus, Y. *Isr. J. Chem.* **1972**, *10*, 659.

Contribution from the Departments of Chemistry, The Ohio State University, Columbus, Ohio 43210,
and The University of Warwick, Coventry CV4 7AL, U.K.

Synthesis and Characterization of Metal Complexes of Nickel, Cobalt, and Iron Having Monomeric 15-Membered Lacunar Cyclidene Ligands, with a Representative Crystal Structure. Dioxygen Binding by the Cobalt Complexes

Rudolf Thomas, Carol M. Fendrick, Wang-Kan Lin, Mark W. Glogowski, Madhav Y. Chavan,
Nathaniel W. Alcock,* and Daryle H. Busch*

Received November 10, 1987

Lacunar nickel(II) complexes of 15-membered cyclidene ligands, having $(CH_2)_n$ (n = 5–8, 12) or *m*-xylylene bridging units, have been synthesized by a template process. The X-ray crystal structure of the derivative with $n = 6$, (2,3,10,11,13,19-hexamethyl-3,10,14,18,21,24-hexaazabicyclo[10.7.6]pentacosa-1,11,13,18,20,24-hexaene-κ^4N)nickel(II) hexafluorophosphate (Vb), $C_{25}H_{42}N_6Ni(PF_6)_2$, has been determined: triclinic, $P\bar{1}$, a = 10.406 (2) Å, b = 14.044 (4) Å, c = 14.251 (4) Å, α = 91.14 (2)°, β = 109.38 (2)°, γ = 111.11 (2)°, Z = 2, and refined to R = 0.096 for 5095 $I > 3\sigma(I)$ data. The ligand salts have been prepared by demetalation of the nickel(II) complexes with HCl(g). Corresponding cobalt(II) complexes and an iron(II) complex have been prepared. The K_{O_2} values for the cobalt(II) complexes were obtained in acetonitrile/1.5 M *N*-methylimidazole.

Introduction

The development of model complexes for heme proteins that can provide insight into the factors important to enhancement of the ability to bind dioxygen presents a continuing challenge.[1-3] For example, the works of Collman[4] and Baldwin[5] have emphasized steric factors, while Traylor[6] has examined electronic factors in the binding of small ligands to heme type units. The cyclidene complexes, which have general structure I, are of interest as totally synthetic (nonporphyrin) models of heme proteins. The overall saddle shape of these complexes (structure II, X = $(CH_2)_3$) provides a cavity within which small ligands can be bound, dioxygen in the cases of the cobalt(II) and iron(II) complexes. Previous reports have shown that these cobalt(II)[7] and iron(II)[8,9]

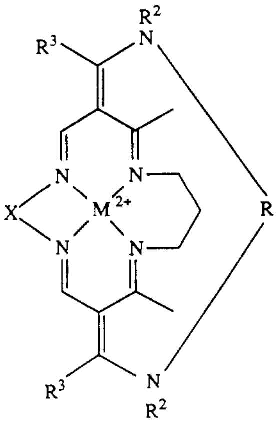

I

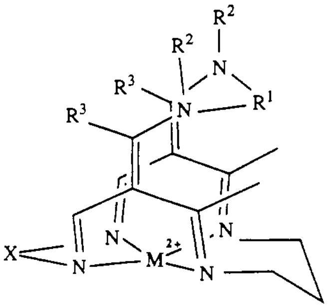

II

---

* To whom correspondence should be addressed: N.W.A., The University of Warwick; D.H.B., The Ohio State University.

(1) Suslick, K. S.; Reinert, T. R. *J. Chem. Educ.* **1985**, *62*, 974.
(2) Collman, J. P.; Halbert, T. R.; Suslick, K. S. In *Metal Ion Activation of Dioxygen*; Spiro, T. B., Ed.; Wiley: New York, 1980; pp 1–72.
(3) Busch, D. H. *Crit. Care Medicine* **1982**, *10*, 246.
(4) Collman, J. P. *Acc. Chem. Res.* **1977**, *10*, 265.
(5) (a) Almog, J.; Baldwin, J. E.; Huff, J. *J. Am. Chem. Soc.* **1975**, *97*, 227. (b) Almog, J.; Baldwin, J. E.; Dyer, R. L.; Peters, M. *Ibid.* **1975**, *97*, 226.
(6) Traylor, T. G.; White, D. K.; Campbell, D. H.; Berzinis, A. P. *J. Am. Chem. Soc.* **1981**, *103*, 4932.
(7) Stevens, J. C.; Busch, D. H. *J. Am. Chem. Soc.* **1980**, *102*, 3285.

0020-1669/88/1327-2534$01.50/0

Scheme I

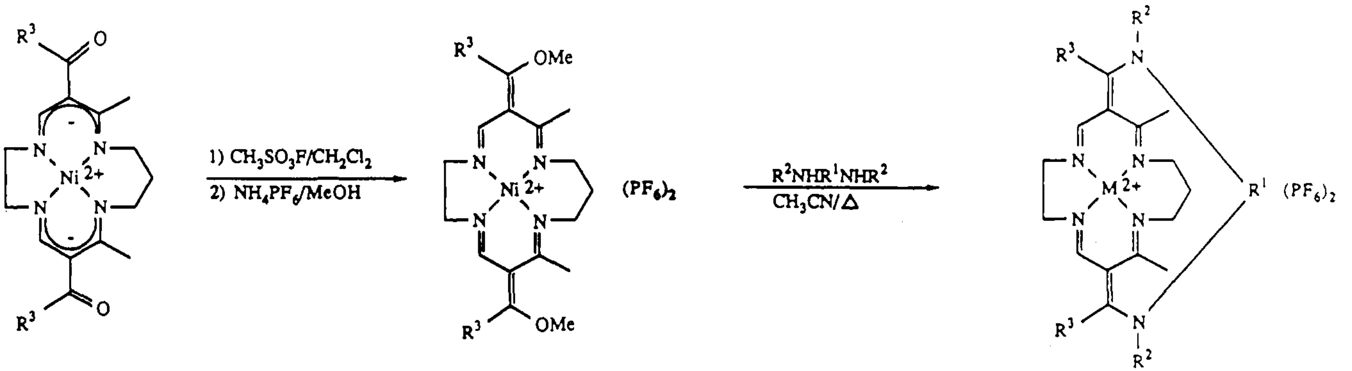

III

IV

V: M= Ni
VI: M= Co
VII: M= Fe

Lacunar Cyclidene Complexes. (R^3 = CH_3)

Ni	Co	Fe	R^1	R^2
Va	VIa		$(CH_2)_5$	CH_3
Vb	VIb		$(CH_2)_6$	CH_3
Vc	VIc		$(CH_2)_7$	CH_3
Vd	VId		$(CH_2)_8$	CH_3
Ve	VIe		$(CH_2)_{12}$	CH_3
Vf	VIf	VII	m-xylylene	CH_3
Vg			$(CH_2)_5$	H
Vh			m-xylylene	H

complexes are unusually good dioxygen carriers. The synthesis of cyclidene ligands with a variety of R^1, R^2, and R^3 groups has allowed both steric and electronic effects to be examined.[10-12]

The variation in the size of the parent cyclidene ring has not been fully explored. In structure I this is achieved by altering the moiety labeled as X. In the present study X has been changed to $(CH_2)_2$, producing a 15-membered cyclidene, whereas all previous studies on the iron(II) and cobalt(II) complexes have dealt with the 16-membered cyclidene (X = $(CH_2)_3$). A single nickel(II) complex containing such a 15-membered cyclidene has been reported.[11]

Results and Discussion

Synthesis and Characterization of the Nickel(II) Complexes. The nickel(II) cyclidene complexes ($R^3 = CH_3$ in all cases) were synthesized as outlined in Scheme I. The synthesis of intermediate IV has previously been reported.[13,14] The reaction of IV with the appropriate diamine results in the formation of the desired cyclidene complexes V in yields from 4 to 33%. When the bridging diamine is primary, R^2 = H, a second product is formed; it is believed to be a dimeric complex similar to those observed with the similar 16-membered macrocycles.[10] Attempts to synthesize complexes with a tetramethylene bridge (structure V, $R^1 = (CH_2)_4$) failed. This behavior differs sharply from that of the 16-membered system where bridges as short as trimethylene (structure V, $R^1 = (CH_2)_3$) have been synthesized successfully.[15]

The monomeric complexes have been characterized by elemental analysis, infrared and ^{13}C NMR spectroscopy, and electrochemical studies. The infrared spectra show a few characteristic features. When a secondary amine (R^1 = H) is present, a sharp N–H stretching absorption is observed in the vicinity of 3400 cm^{-1}. This band is not present when $R^2 = CH_3$. Bands due to C=C and C=N are found in the vicinity of 1500–1600 cm^{-1}. The spectra of the complexes also show broad strong bands at 840 and 540 cm^{-1} that are characteristic of PF_6^- salts.

The ^{13}C NMR data are presented in Table I. These assignments were made in part with the aid of previous ^{13}C-labeling studies carried out on a 16-membered-ring derivative[16] and by off-resonance decoupling experiments. These spectroscopic studies support the expected chemical structures.

Electrochemical results determined in acetonitrile in the presence of 1.5 M *N*-methylimidazole are summarized in Table II. The first oxidation process is believed to correspond to the nickel(II)/nickel(III) couple.[18] A second oxidation occurs around +1.1 V and is usually reversible. This process probably involves ligand oxidation. The nickel(II)/nickel(III) oxidation for the 15-membered macrocycles occurs at a lower potential than it does for corresponding 16-membered-ring species.[10] This is consistent with the expectation that the smaller macrocycle places more electron density on the metal ion.[19]

Structure of Complex Having X = $(CH_2)_2$, $R^1 = (CH_2)_6$, and $R^2 = R^3 = CH_3$ (Vb). The atom-numbering scheme and structure of the cation are shown in Figure 1. The complex exhibits the typical saddle shape that has been well documented for the 16-membered lacunar cyclidene complexes.[20] The six-membered chelate ring formed by N(1), Ni, N(2), C(20), C(21), and C(22) is in the boat conformation. The metal atom is positioned 0.03

---

(8) (a) Herron, N.; Zimmer, L. L.; Grzybowski, J. J.; Olszanski, D. J.; Jackels, S. C.; Callahan, R. W.; Cameron, J. H.; Christoph, G. G.; Busch, D. H. *J. Am. Chem. Soc.* **1983**, *105*, 6585. (b) Herron, N.; Busch, D. H. *J. Am. Chem. Soc.* **1981**, *103*, 1236.

(9) Herron, N.; Cameron, J. H.; Neer, G. L.; Busch, D. H. *Ibid.* **1983**, *105*, 298.

(10) Busch, D. H.; Jackels, S. C.; Callahan, R. C.; Grzybowski, J. J.; Zimmer, L. L.; Kojima, M.; Olszanski, D. J.; Schammel, W. P.; Stevens, J. C.; Holter, K. A.; Mocak, J. *Inorg. Chem.* **1981**, *20*, 2834.

(11) Daszkiewicz, B. K.; Kojima, M.; Cameron, J. H.; Herron, N.; Chavan, M. Y.; Jircitano, A. J.; Coltrain, B. K.; Neer, G. L.; Alcock, N. W.; Busch, D. H. *Inorg. Chem.* **1984**, *23*, 903.

(12) Busch, D. H.; Olszanski, D. J.; Stevens, J. C.; Schammel, W. P.; Kojima, M.; Herron, N.; Zimmer, L. L.; Holter, K. A.; Mocak, J. *J. Am. Chem. Soc.* **1981**, *103*, 1472.

(13) Schammel, W. P.; Zimmer, L. L.; Busch, D. H. *Inorg. Chem.* **1980**, *19*, 3159.

(14) Hipp, C. J.; Corfield, P. W. R.; Mokren, J. D.; Busch, D. H. *J. Am. Chem. Soc.* **1973**, *95*, 4465.

(15) Herron, N.; Chavan, M. Y.; Busch, D. H. *J. Chem. Soc., Dalton Trans.* **1984**, 1491.

(16) Takeuchi, K. J.; Busch, D. H.; Alcock, N. *J. Am. Chem. Soc.* **1983**, *105*, 4261.

(17) Chavan, M. Y.; Meade, T. J.; Busch, D. H.; Kuwana, T. *Inorg. Chem.* **1986**, *25*, 314.

(18) Lovecchio, F. V.; Gore, E. S.; Busch, D. H. *J. Am. Chem. Soc.* **1974**, *96*, 3109.

(19) Hung, Y.; Martin, L. Y.; Jackels, S. C.; Tait, M. A.; Busch, D. H. *J. Am. Chem. Soc.* **1977**, *99*, 4029.

(20) Alcock, N. W.; Lin, W.-K.; Jircitano, A.; Mokren, J. D.; Corfield, P. W. R.; Johnson, G.; Novotnak, G.; Cairns, C.; Busch, D. H. *Inorg. Chem.* **1987**, *26*, 440.

Table I. ^{13}C NMR Data for the Nickel(II) Complexes

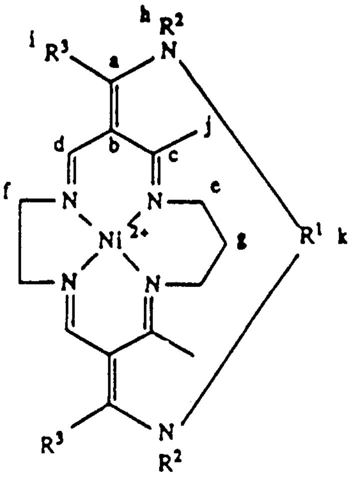

	a	*b*	*c*	*d*	*e*	*f*	*g*	*h*	*i*	*j*	*k*
Ia	176.0	167.1	157.8	112.2	58.5	55.7	31.0	51.8	22.0	20.6	42.9, 28.3, 24.2
Ib	176.1	167.5	158.9	111.1	57.8	55.9	31.3	51.8	22.1	20.8	41.3, 26.3, 25.6
Ic	177.7	167.1	158.2	110.9	57.4	56.3	31.5	52.2	22.4	20.7	40.3, 28.1, 27.7, 25.7
Id	177.1	166.9	158.7	110.4	57.9	56.6	31.7	52.2	22.4	21.0	40.5, 26.1, 25.7, 23.5
Ie	181.6	164.6	155.3	108.5	59.2	57.3	30.8	47.5	25.3	19.8	41.3, 30.3, 28.5, 26.7
If	177.0	167.1	157.8	114.2	62.4	55.7	31.0	52.2	22.3	21.0	45.7, 137.6, 130.3, 125.7, 125.2
Ig	173.5	168.8	159.2	111.3	55.8	51.7	30.6		22.3	21.0	48.1, 30.4, 23.9

Table II. Electrochemical Data[a] for Nickel(II) Complexes of 15- and 16-Membered Lacunar Cyclidene Ligands in Acetonitrile (0.1 M $(TBA)BF_4$)

			[15]		[16]
compd	R^2	R^1	$E_{1/2}$, V	ΔE,[b] mV	$E_{1/2}$, V
Vb	CH_3	$(CH_2)_6$	0.68	60	0.76
Vd	CH_3	$(CH_2)_8$	0.65	75	0.77
Ve	CH_3	$(CH_2)_{12}$	0.53	80	0.74
Vf	CH_3	*m*-xylylene	0.71*	75	0.78
Vg	H	$(CH_2)_5$	0.80*	80	0.85
Vh	H	*m*-xylylene	0.85*	80	0.93

[a] Measured by using a rotating Pt-disk electrode vs $Ag/AgNO_3$ (0.1 M) in acetonitrile. Values for $[Ni(15)]^{3+/2+}$ and $[Ni(16)]^{3+/2+}$, except for those identified by asterisks, were reported previously in ref 10 and 17. [b] $|E_{3/4} - E_{1/4}|$.

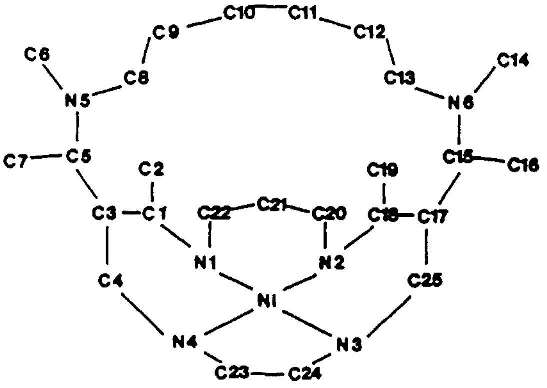

Figure 1. Atom-numbering scheme for the structure of Vb ($R^1 = (CH_2)_6$, $R^2 = R^3 = CH_3$).

Å out of the plane defined by the four coordinating nitrogen atoms on the side opposite the bridge. The complex has the lid-off conformation,[8,10,21] which results in a wide but shallow cavity. Although, both this structure and that of the 16-membered analogue have lid-off bridge conformations, it is interesting to note that the cavity of the 15-membered-ring derivative is both wider and lower.[22,23] This is clearly shown by a comparison. The angle between the N(1)-N(4)-C(1)-C(4) plane and the N(2)-N-(3)-C(18)-C(25) plane is 108.1°, and that between the C(1)-C(3)-C(4) plane and the C(18)-C(17)-C(25) plane is 72.2°. These are substantially larger than the corresponding values in the corresponding complex with a 16-membered ring (98.8 and 44.5°).[22] The void width, as defined by the distances from C(3) to C(17), from C(5) to C(15), and from N(5) to N(6), varies between 5.55, 7.23, and 7.12 Å, respectively, 0.3–0.6 Å wider than the cavity in the 16-membered-ring complex. The cavity height, defined by the average distances from the metal to C(10) and C(11) (the carbon atoms in the middle of the polymethylene chain) is 4.63 Å (compared to 5.14 Å). As can be seen from Figure 2, this comparatively low cavity is further constricted by the hydrogen atoms of these methylene groups.

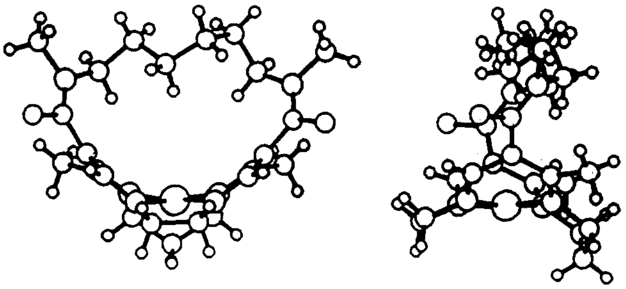

Figure 2. Structural representations of complex Vb ($R^1 = (CH_2)_6$, $R^2 = R^3 = CH_3$).

The polymethylene bridge of the complex has the same conformation as those of the 16-membered cyclidene complexes.[22] From C(8) to C(13), the single bonds of the five sp^3 carbons show a g-a-g-g-g conformation (g = gauche, a = anti). Detailed studies[22] have shown that this conformation not only offers an appropriate length to span the two sides of the macrocycle and give a good angle to connect the two nitrogen atoms (N(5) and N(6)) in the vinyl group but also results in a lower total energy within the bridge chain itself because of the anti and gauche conformations.

Selected bond lengths and bond angles are given in Table III. Most values are standard, but delocalization is clearly indicated for the two unsaturated rings.

---

(21) Herron, N.; Nosco, D. L.; Busch, D. H. *Inorg. Chem.* **1983**, *22*, 2970.
(22) Alcock, N. W.; Lin, W.-K.; Busch, D. H., manuscript in preparation.
(23) Chavan, M. Y. Ph.D. Thesis, The Ohio State University, Columbus, OH, 1983.

Table III. Selected Bond Lengths (Å) and Bond Angles (deg)

Ni-N(1)	1.896 (6)	Ni-N(2)	1.892 (6)
Ni-N(3)	1.854 (6)	Ni-N(4)	1.857 (6)
N(1)-C(1)	1.280 (7)	N(1)-C(22)	1.488 (7)
N(2)-C(18)	1.296 (8)	N(2)-C(20)	1.479 (8)
N(3)-C(24)	1.455 (15)	N(3)-C(25)	1.296 (10)
N(4)-C(4)	1.296 (8)	N(4)-C(23)	1.445 (14)
N(5)-C(5)	1.303 (10)	N(5)-C(6)	1.479 (8)
N(5)-C(8)	1.475 (10)	N(6)-C(13)	1.481 (10)
N(6)-C(14)	1.480 (11)	N(6)-C(15)	1.300 (10)
C(1)-C(2)	1.496 (11)	C(1)-C(3)	1.450 (9)
C(3)-C(4)	1.408 (11)	C(3)-C(5)	1.428 (7)
C(5)-C(7)	1.509 (12)	C(8)-C(9)	1.517 (11)
C(9)-C(10)	1.530 (17)	C(10)-C(11)	1.483 (16)
C(11)-C(12)	1.548 (16)	C(12)-C(13)	1.465 (9)
C(15)-C(16)	1.500 (11)	C(15)-C(17)	1.435 (9)
C(17)-C(18)	1.445 (9)	C(17)-C(25)	1.403 (12)
C(18)-C(19)	1.507 (11)	C(20)-C(21)	1.526 (10)
C(21)-C(22)	1.482 (9)	C(23)-C(24)	1.469 (13)
N(1)-Ni-N(2)	95.1 (2)	N(1)-Ni-N(3)	171.9 (2)
N(2)-Ni-N(3)	91.0 (3)	N(1)-Ni-N(4)	90.3 (3)
N(2)-Ni-N(4)	172.9 (2)	N(3)-Ni-N(4)	83.2 (3)
Ni-N(1)-C(1)	122.6 (4)	Ni-N(1)-C(22)	117.3 (4)
C(1)-N(1)-C(22)	120.1 (6)	Ni-N(2)-C(18)	122.9 (4)
Ni-N(2)-C(20)	118.4 (4)	C(18)-N(2)-C(20)	118.7 (6)
Ni-N(3)-C(24)	113.7 (5)	Ni-N(3)-C(25)	121.8 (6)
C(24)-N(3)-C(25)	122.1 (7)	Ni-N(4)-C(4)	121.1 (6)
Ni-N(4)-C(23)	113.7 (5)	C(4)-N(4)-C(23)	121.9 (7)
C(5)-N(5)-C(6)	122.0 (6)	C(5)-N(5)-C(8)	124.9 (5)
C(6)-N(5)-C(8)	112.7 (6)	C(13)-N(6)-C(14)	112.4 (7)
C(13)-N(6)-C(15)	125.2 (6)	C(14)-N(6)-C(15)	122.3 (6)
N(1)-C(1)-C(2)	119.9 (6)	N(1)-C(1)-C(3)	122.5 (6)
C(2)-C(1)-C(3)	117.1 (5)	C(1)-C(3)-C(4)	118.9 (5)
C(1)-C(3)-C(5)	125.1 (7)	C(4)-C(3)-C(5)	115.9 (6)
N(4)-C(4)-C(3)	124.2 (7)	N(5)-C(5)-C(3)	123.4 (6)
N(5)-C(5)-C(7)	118.0 (5)	C(3)-C(5)-C(7)	118.6 (7)
N(5)-C(8)-C(9)	112.8 (6)	C(8)-C(9)-C(10)	112.8 (8)
C(9)-C(10)-C(11)	115.9 (12)	C(10)-C(11)-C(12)	112.3 (9)
C(11)-C(12)-C(13)	119.3 (9)	N(6)-C(13)-C(12)	112.1 (6)
N(6)-C(15)-C(16)	117.7 (6)	N(6)-C(15)-C(17)	121.9 (6)
C(16)-C(15)-C(17)	120.6 (7)	C(15)-C(17)-C(18)	123.4 (7)
C(15)-C(17)-C(25)	117.1 (6)	C(18)-C(17)-C(25)	119.4 (6)
N(2)-C(18)-C(17)	121.9 (6)	N(2)-C(18)-C(19)	119.5 (6)
C(17)-C(18)-C(19)	118.2 (6)	N(2)-C(20)-C(21)	110.7 (6)
C(20)-C(21)-C(22)	112.5 (5)	N(1)-C(22)-C(21)	112.0 (6)
N(4)-C(23)-C(24)	110.0 (9)	N(3)-C(24)-C(23)	110.1 (9)
N(3)-C(25)-C(17)	124.6 (7)		

Table IV. Electrochemical Data[a] for Cobalt(II) Complexes of 15- and 16-Membered Lacunar Cyclidene Ligands in Acetonitrile (0.1 M (TBA)BF$_4$)

compd	R^1	[15][b] $E_{1/2}$, V	[15][b] ΔE, mV	[16] $E_{1/2}$, V
VIb	(CH$_2$)$_6$	0.21	70	0.20[c]
VIc	(CH$_2$)$_7$	0.13	110	0.08[c]
VId	(CH$_2$)$_8$	0.06	80	0.05[c]
VIe	(CH$_2$)$_{12}$	−0.03*	70	
VIf	*m*-xylylene	0.28*	70	0.31*[b]

[a] R^2 = R^3 = CH$_3$. Potentials vs Ag/AgNO$_3$ (0.1 M). Values for [Co(15)]$^{3+/2+}$ and [Co(16)]$^{3+/2+}$, except for those identified by an asterisk, were first reported in ref 17. [b] Pt-disk electrode. [c] Rotating Pt-disk electrode.

Synthesis of Cobalt(II) and Iron(II) Complexes. The ligand salts of the complexes were prepared by demetalation of the nickel(II) complexes with HCl(g) in acetonitrile solvent.[12] They were combined with cobalt(II) acetate in the presence of sodium acetate trihydrate in methanol solution to give the cobalt complexes in 50–60% yield.

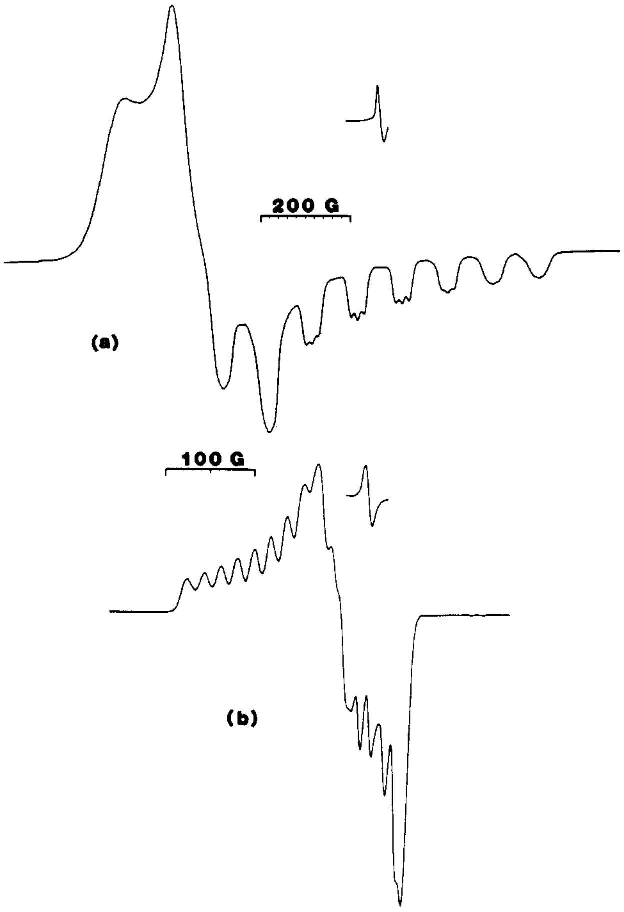

Figure 3. ESR spectra in 1.5 M *N*-MIM/CH$_3$CN solution at −196 °C of (a) the cobalt(II) complex VIc (structure VI, R^1 = (CH$_2$)$_7$, R^2 = R^3 = CH$_3$) and (b) its dioxygen adduct.

The cobalt complexes were characterized by elemental analysis, infrared spectroscopy, and electrochemistry. The infrared spectra were similar to those of the nickel complexes. The electrochemical data for the Co^{2+}/Co^{3+} couple are shown in Table IV. The $E_{1/2}$ values for the complexes of the 15-membered macrocycles are more anodic than those for the corresponding 16-membered macrocycles with the exception of the *m*-xylylene derivative.[23]

The iron complex of the ligand salt derived from Vf was successfully prepared in excellent yield by the reaction with Fe(py)$_2$Cl$_2$ and triethylamine in acetonitrile. This compound was characterized by elemental analysis. It is potentially of significance as an oxygen carrier and is the subject of further study.

ESR and K_{O_2} Measurements. ESR spectra of the unoxygenated cobalt(II) complexes confirm the five-coordinate nature of the species in solution (Table V, Figure 3a). These ESR spectra display rhombic patterns with $g_1 \cong 2.4$, $g_2 \cong 2.3$, and $g_3 \cong 2.0$. The parallel component is split into eight lines ($A_\parallel \cong 104$ G) from coupling to ^{59}Co ($I = {}^7/_2$) and superhyperfine coupling to the ^{14}N atom ($I = 1$) of the axial *N*-methylimidazole (*N*-MIM) is observed in some spectra ($a_N \cong 14$ G).

Table V. ESR Parameters[a] for 15-Membered-Cyclidene Complexes (R^2 = R^3 = CH$_3$) of Cobalt(II) and Their Dioxygen Adducts

		cobalt(II) complexes					dioxygen adducts			
compd	R^1	g_1	g_2	g_3	$A_\parallel$, G	a_N, G	$g_\parallel$	$A_\parallel$, G	$g_\perp$	$A_\perp$, G
VIb	(CH$_2$)$_6$	2.404	2.287	2.008	103.6	14.0	2.087	18.0	1.999	12.0
VIc	(CH$_2$)$_7$	2.417	2.276	2.004	101.4	13.9	2.086	18.5	2.000	12.1
VId	(CH$_2$)$_8$	2.411	2.278	2.006	100.3	*b*	2.086	17.8	1.999	11.6
VIe	(CH$_2$)$_{12}$	2.445	2.284	2.005	107.1	14.3	2.087	18.2	1.998	11.8
VIf	*m*-xylylene	2.393	2.287	2.009	103.2	*b*	2.089	18.8	2.000	12.5

[a] 1.5 M *N*-MIM/acetonitrile frozen glass at −196 °C. [b] Superhyperfine splittings insufficiently resolved to determine a_N.

Table VI. Equilibrium Data for 15- and 16-Membered-Cyclidene Complexes ($R^2 = R^3 = CH_3$) of Cobalt(II) at 20 °C in Acetonitrile/1.5 M *N*-MIM

complex	R^1	K_{O_2}, $Torr^{-1}$ [15]	K_{O_2}, $Torr^{-1}$ [16]
VIf	*m*-xylylene	*a*	*b*
VIa	$(CH_2)_5$	0.003	0.0094[c]
VIb	$(CH_2)_6$	0.52	0.155[c]
VIc	$(CH_2)_7$	1.32	0.62
VId	$(CH_2)_8$	5.2	0.65
VIe	$(CH_2)_{12}$	very large	

[a] Very small even at −40 °C. [b] K_{O_2} = 0.0012 at −30 °C. [c] First reported in ref 7.

On exposure of the solutions to 760 Torr of dioxygen, ESR spectra characteristic of the 1:1 dioxygen adducts are observed (Table V, Figure 3b), with $g_\parallel \cong 2.09$ and $g_\perp \cong 2.00$. The ESR spectral patterns of the dioxygen adducts are similar for the series, and the magnitude of the hyperfine coupling constants $A_\parallel$ and $A_\perp$ show little variation from ~18 and ~12 G, respectively.

The K_{O_2} values for the 15- and 16-membered-ring complexes are listed in Table VI. For bridges longer than $(CH_2)_6$ the K_{O_2} values for the 15-membered-ring complexes in acetonitrile/1.5 M *N*-MIM are greater than those for the 16-membered analogues,[24,25] while for R^1 = *m*-xylylene and $(CH_2)_5$ the opposite is true. This inconsistent behavior does not parallel the electrochemical data, which would suggest higher K_{O_2} values for the 16-membered-cyclidene derivatives with the exception, once again, of the *m*-xylylene derivatives.[26] Because of the complexities of the subject, the basis for the use of the electrochemical results must be clarified.

For the nickel(II) complexes, the metal ion couple has generally been found to be independent of the nature of the bridge among the lacunar complexes.[12] Further, the potential of the Co^{III}/Co^{II} couple is quite sensitive to the bridge length, a relationship attributed to the importance of binding a ligand within the cavity of the oxidized member of the couple.[17,23] Thus, the Ni^{III}/Ni^{II} potentials for the 16-membered cyclidenes having ring sizes ranging from tetramethylene to dodecamethylene show essentially no systematic variation and, indeed, are very nearly the same.[12,17] Consequently, the potentials of the nickel complexes should be more indicative of the electronic consequences of changing the size of the parent macrocycle. For nickel, the potential is always more cathodic for the 15-membered-macrocyclic-ring derivatives than the 16-membered ones, indicating increased electron density for the former. For cobalt, the opposite is true. It is suggested that this results from the fact that a longer bridge is required to produce the equivalent lacuna for the derivatives of the 15-membered cyclidene. Consequently, for a given bridge size, the cavity is more available to the sixth ligand in the case of the 16-membered cyclidene, and this stabilizes the oxidized state. Clearly, the nickel electrochemical data are more appropriate for predicting the relative dioxygen affinities of the complexes when the size of the parent macrocycle is changed among lacunar complexes.

Returning to the inconsistent behavior of the dioxygen affinity as the bridging group changes among 15-membered-cyclidene complexes of cobalt, we believe the most probable explanation is the tendency to shift from the saddle shape for the 16-membered cyclidene toward a more nearly planar conformation for the 15-membered cyclidene.[20] This would yield a concomitant decrease in cavity size for the same bridging group. Such a change might have a particularly dramatic effect on the complexes with short bridges. This is borne out by the wider and lower cavity in the structure of Vb and by our failure in attempts to prepare the 15-membered-cyclidene complex having the shorter $(CH_2)_4$ bridge, a synthesis that is routine for the 16-membered-cyclidene system.

Table VII. Summary of Crystallographic Data

formula	$NiC_{25}H_{39}N_6P_2F_{12}\cdot C_2H_3N$	space group	$P\bar{1}$
		D_{calcd}, g cm^{-3}	1.49
mol wt	813.3	D_{measd}, g cm^{-3}	1.41
system	triclinic	cryst size, mm	0.9 × 0.6 × 0.6
a, Å	10.406 (2)	μ, cm^{-1}	7.1
b, Å	14.044 (4)	radiation (λ, Å)	Mo Kα (0.71069)
c, Å	14.251 (4)	2θ max, deg	50
α, deg	91.14 (2)	no. of data measd	6412
β, deg	109.38 (2)	no. of data with $I/\sigma(I) > 3$	5095
γ, deg	111.11 (2)		
V, Å	1809.7 (8)	*R*	0.096
Z	2	R_w	0.107

The higher dioxygen affinities found for the 15-membered-cyclidene complexes for longer bridging groups, as compared to the corresponding 16-membered-cyclidene complexes, agrees with the usual correlation between O_2 affinity and redox potential, again, on the basis of the data for the corresponding nickel complexes. The exceptional behavior of the *m*-xylylene-bridged complexes remains unexplained. The fact that both metal couples shift in the direction predicted by the electron density dependence of the oxygen affinity may derive from the broader, more constricting benzene group in the bridge. In the presence of the *m*-xylylene bridge, the solvent may be denied access to the cavity for all metal ions; this would eliminate the interaction that appears to distinguish the behavior of the two electrode couples.[17]

Experimental Section

Physical Measurements. Infrared spectra were obtained by using either Nujol mulls or KBr pellets on a Perkin-Elmer 283B infrared spectrophotometer. Ultraviolet and visible spectra were obtained on a Cary Model 17D recording spectrophtoometer or a Varian 2300 spectrophotometer. ESR spectra were measured on a Varian E-112 spectrometer in the X band at 9.3 GHz on frozen glasses (−196 °C), and the *g* values are quoted relative to external pitch (0.1%, *g* = 2.0028). Dioxygen-binding measurements were obtained by the method of Stevens.[27] The cell temperature and dioxygen pressure were controlled as described earlier.[8a] Electrochemical measurements were carried out as reported previously.[12] Air-sensitive samples were prepared in a Vacuum Atmospheres inert-atmosphere box under dioxygen-free dinitrogen. Elemental analyses were performed by Galbraith Laboratories, Inc., Knoxville, TN.

Crystal Structure Analysis. A summary of crystallographic data is given in Table VII.

X-ray Data Collection and Reduction. Data were collected with a Syntex $P2_1$ four-circle diffractometer. The maximum 2θ was 50°, with scan range +0.9° (2θ) around the $K\alpha_1$–$K\alpha_2$ angles and scan speed 2–29° min^{-1}, depending on the intensity of a 2-s prescan; backgrounds were measured at each end of the scan for one-fourth of the scan time. Three standard reflections were monitored every 200 reflections and showed slight changes during data collection; the data were rescaled to correct for this. Density was measured by flotation. Unit cell dimensions and standard deviations were obtained by a least-squares fit to 15 high-angle reflections. In refinement, 5095 observed reflections ($I/\sigma(I) > 3.0$) from 6412 recorded reflections were used and corrected for Lorentz, polarization, and absorption effects, the last with ABSCOR;[28] maximum and minimum transmission factors were 0.87 and 0.80. There were no systematic absences.

Structure Solution and Refinement. The heavy atom was located by Patterson techniques, and the light atoms were then found on successive Fourier syntheses. Hydrogen atoms were inserted at calculated positions with fixed isotropic temperature factors. At a late stage, a solvent molecule was found. Although its temperature factors were high, refinement of its occupancy converged at 1.07 (1). Final refinement was by least-squares methods in cascaded large blocks with anisotropic temperature factors for non-hydrogen and non-solvent atoms. The largest peak on the final Fourier synthesis was 2 e $Å^{-3}$ near the Ni atom. A weighting scheme of the form $w = 1/(\sigma^2(F) + gF^2)$ with $g = 0.002$ was used and shown to be satisfactory by a weight analysis. The final *R*

---

(24) Stevens, J. C.; Jackson, P. J.; Schammel, W. P.; Christoph, G. G.; Busch, D. H. *J. Am. Chem. Soc.* **1980**, *102*, 3283.

(25) Jackson, P. J. Ph.D. Thesis, The Ohio State University, Columbus, OH, 1981.

(26) (a) Carter, M. J.; Egelhardt, L. M.; Rillema, D. P.; Basolo, F. *J. Chem. Soc., Chem. Commun.* **1973**, 810. (b) Carter, M. J.; Rillema, D. P.; Basolo, F. *J. Am. Chem. Soc.* **1974**, *96*, 392.

(27) Stevens, J. C. Ph.D. Thesis, The Ohio State University, Columbus, OH, 1979.

(28) Alcock, N. W. *Crystallographic Computing*; Ahmed, F., Ed.; Munksgaard: Copenhagen, 1970.

Table VIII. Atom Coordinates ($\times 10^4$) and Temperature Factors ($Å^2 \times 10^3$)

atom	*x*	*y*	*z*	U_{eq}[a]
Ni	183 (1)	3118 (1)	1775 (1)	21 (1)
P(1)	−683 (2)	2311 (1)	6239 (1)	45 (1)
P(2)	4176 (2)	2275 (2)	365 (2)	53 (1)
F(11)	−1515 (6)	1640 (4)	5151 (4)	81 (3)
F(12)	−1576 (7)	3023 (4)	5902 (4)	95 (3)
F(13)	570 (6)	2997 (4)	5875 (4)	85 (3)
F(14)	231 (7)	1608 (4)	6595 (4)	89 (3)
F(15)	179 (6)	3004 (4)	7313 (3)	84 (3)
F(16)	−1924 (7)	1607 (5)	6596 (5)	103 (4)
F(21)	3322 (6)	2525 (4)	1009 (4)	76 (3)
F(22)	5042 (6)	2050 (5)	−283 (4)	91 (3)
F(23)	2682 (6)	1779 (5)	−575 (4)	105 (3)
F(24)	4435 (7)	3357 (4)	4 (5)	97 (3)
F(25)	3821 (9)	1157 (5)	676 (6)	122 (5)
F(26)	5642 (7)	2726 (7)	1314 (5)	136 (4)
N(101)	5753 (16)	−92 (10)	3014 (11)	182 (6)
C(101)	6186 (12)	121 (8)	2357 (9)	117 (4)
C(102)	6663 (14)	380 (9)	1586 (9)	139 (4)
N(1)	768 (5)	3687 (4)	716 (4)	41 (2)
N(2)	202 (5)	1810 (4)	1457 (4)	39 (2)
N(3)	−210 (6)	2741 (4)	2922 (4)	46 (3)
N(4)	265 (6)	4386 (4)	2253 (4)	51 (3)
N(5)	4872 (5)	6130 (4)	2110 (4)	49 (2)
N(6)	3322 (6)	1321 (4)	3943 (4)	47 (3)
C(1)	1735 (6)	4602 (5)	839 (4)	44 (3)
C(2)	2227 (9)	4977 (6)	−8 (5)	67 (4)
C(3)	2248 (7)	5355 (4)	1729 (5)	46 (3)
C(4)	1341 (7)	5241 (5)	2298 (5)	52 (3)
C(5)	3658 (7)	6196 (4)	2116 (5)	51 (3)
C(6)	6296 (8)	7035 (6)	2455 (6)	77 (4)
C(7)	3753 (9)	7217 (6)	2556 (7)	84 (4)
C(8)	5036 (7)	5156 (5)	1901 (5)	56 (3)
C(9)	5791 (9)	4800 (6)	2850 (6)	78 (4)
C(10)	4761 (14)	4299 (9)	3414 (7)	113 (7)
C(11)	5302 (13)	3725 (8)	4212 (8)	113 (6)
C(12)	5400 (9)	2745 (6)	3778 (7)	90 (5)
C(13)	4037 (8)	1841 (6)	3249 (5)	62 (4)
C(14)	4210 (9)	837 (6)	4648 (6)	72 (4)
C(15)	2089 (7)	1317 (4)	3981 (4)	44 (3)
C(16)	1715 (10)	978 (6)	4883 (5)	70 (4)
C(17)	1107 (7)	1624 (5)	3195 (4)	45 (3)
C(18)	745 (6)	1317 (4)	2136 (4)	42 (3)
C(19)	833 (8)	321 (5)	1814 (5)	60 (3)
C(20)	−404 (8)	1342 (5)	384 (4)	55 (3)
C(21)	−1066 (7)	2007 (5)	−288 (4)	55 (3)
C(22)	69 (7)	3017 (5)	−285 (4)	56 (3)
C(23)	−632 (11)	4311 (6)	2857 (7)	89 (5)
C(24)	−892 (11)	3341 (7)	3275 (7)	89 (5)
C(25)	412 (7)	2201 (5)	3490 (5)	51 (3)

[a] $U_{eq} = {}^1/_3 \sum_i \sum_j U_{ij} a^*_i a^*_j \vec{a}_i \cdot \vec{a}_j$.

values were $R = 0.096$ and $R_w = 0.107$. These relatively high R values are explained by the partial disorder of the PF_6 groups, which leads to the presence of numerous residual peaks (about 1 e $Å^{-3}$ height) around the PF_6 ions. Computing was done with the SHELXTL system on a Data General NOVA3 computer. Scattering factors in the analytical form and anomalous dispersion factors were taken from ref 29. Final atomic coordinates are given in Table VIII, and selected bond lengths and angles in Table III. A listing of observed and calculated structure factors, anisotropic temperature factors, bond lengths and angles, hydrogen positions, and a packing diagram are available as supplementary material.

Materials. Acetonitrile, methanol, and benzene were dried over calcium hydride. Methylene chloride, diethyl ether, acetone (all reagent grade), and acetonitrile-d^3 (Cambridge Isotopes) were used without further purification. Neutral alumina (Fischer Scientific) and CM Sephadex (Sigma) were used as received; vide infra. Ammonium hexafluorophosphate (Aldrich) was recrystallized from methanol before use. Cobalt acetate tetrahydrate (Alfa), sodium acetate trihydrate (Mallinkrodt), *N,N'*-dimethyl-1,6-diaminohexane, *N,N'*-dimethyl-1,4-diaminobutane (both from AMES Laboratory), 1,5-diaminopentane, 1,7-diaminoheptane, 1,8-diaminooctane, and 1,12-diaminododecane (all from Aldrich) were used as purchased. Dichlorobis(pyridine)iron(II), $Fe(py)_2Cl_2$, was prepared by a literature method.[30] *N*-methylimidazole (*N*-MIM) was dried over barium oxide. Solvents used in the inert-atmosphere box were degassed in vacuo.

Table IX. Yields of Ligand Salts ($R^2 = R^3 = CH_3$)

demetalated compd	R^1	amt, g (mmol) Ni complex	amt, g (mmol) ligand	% yield
Va	$(CH_2)_5$	0.9 (1.18)	0.9	86
Vb	$(CH_2)_6$	0.5 (0.64)	0.5	86
Vc	$(CH_2)_7$	0.2 (0.25)	0.1	43
Vd	$(CH_2)_8$	0.4 (0.50)	0.2	43
Ve	$(CH_2)_{12}$	0.2 (0.23)	0.1	44
Vf	*m*-xylylene	0.2 (0.25)	0.15	65

Syntheses. (2,11-Dimethyl-3,10-bis(1-methoxyethylidene)-1,5,8,12-tetraazacyclopentadeca-1,4,8,11-tetraene)nickel(II) Hexafluorophosphate (IV). This complex was synthesized according to previously published procedures.[13,14]

α,α'-Bis(methylamino)-*m*-xylene. This secondary diamine was prepared by standard organic chemistry techniques.[31]

***N,N'*-Dimethyldiaminoalkanes.** *N,N'*-Dimethyl-1,5-diaminopentane, *N,N'*-dimethyl-1,7-diaminoheptane, *N,N'*-dimethyl-1,8-diaminooctane, and *N,N'*-dimethyl-1,12-diaminododecane were synthesized by a modification of a literature procedure.[32] Yields were 26%, 42%, 66%, and 71%, respectively. The procedure for the synthesis of *N,N'*-dimethyl-1,5-diaminopentane is given as follows.

A three-necked flask was fitted with a Dean–Stark apparatus. Benzaldehyde (22 mL) and 1,5-diaminopentane (10 g) were placed in the flask along with 100 mL of benzene. The reaction mixture was refluxed for 1 h while product water was collected in the Dean–Stark trap. Dimethyl sulfate (25 g, 19 mL) was added dropwise to the refluxing solution over a period of 1 h, after which two layers formed. The upper benzene layer was discarded. Water, 200 mL, was added to the lower layer, and the solution was refluxed for 1 h. The mixture was extracted with diethyl ether (3 × 50 mL) to remove the benzaldehyde. The aqueous layer was reduced in volume to ~20 mL by rotary evaporation. This concentrated solution was then made alkaline with NaOH (2 g) and extracted with diethyl ether (3 × 50 mL), and the ether solution was dried over $MgSO_4$. Evaporation of the ether solution yielded an oil. Distillation at 2 Torr and 100 °C yielded 34 g (26%) of product.

Synthesis of the Bridged Complexes. The bridged complexes were synthesized by essentially the same procedure that is presented for Va below.

(2,3,9,10,12,18-Hexamethyl-3,9,13,17,20,23-hexaazabicyclo[9.7.6]tetracosa-1,10,12,17,19,23-hexaene-κ⁴*N*)nickel(II) Hexafluorophosphate (Va, $R^1 = (CH_2)_5$, $R^2 = R^3 = CH_3$). Acetonitrile (200 mL) was placed in a dry three-necked, 2-L, round-bottomed flask fitted with a reflux condenser having a drying tube, and the solvent was heated to reflux. Solutions of IV (10 g, 0.027 mol) in 300 mL of acetonitrile and *N,N'*-dimethyl-1,5-diaminopentane (0.027 mol) in 300 mL of acetonitrile were dripped into the stirred, refluxing acetonitrile over a period of 5–6 h by using a polystaltic pump. The reaction produced a very dark solution. The volume of the solution was reduced to ~20 mL with a rotary evaporator. The concentrated solution was chromatographed on neutral alumina by eluting with acetonitrile. This produced a yellow or red fast-moving band followed by, but not separated from, a darker material. The bands were separated as well as possible; the solutions were concentrated and then chromatographed on fresh neutral alumina by eluting with methylene chloride or methylene chloride/acetone. The colored material was collected, taken to dryness on a rotary evaporator, and dissolved in 100 mL of acetone.

The compound was adsorbed onto a small quantity of CM Sephadex in the following manner: Water was added to an acetone solution of the compound until a precipitate formed. The precipitate was redissolved by the addition of acetone to the mixture to give a total solution volume of 300 mL. This solution was passed under vacuum through a 30-mL frit half-filled with CM Sephadex. The light yellow filtrate was further diluted with water (200 mL), and the solution again passed through the CM Sephadex. At this point the filtrate was almost clear.

The CM Sephadex containing the compound was loaded onto the top of a 4 × 20 cm column of CM Sephadex, and a layer of sand was added. Elution with 0.2 M Na_2SO_4 produced a red band followed by a black band with adequate separation. The red band was collected, and the compound was precipitated with NH_4PF_6. When necessary, the com-

---

(29) *International Tables for X-Ray Crystallography*; Kynoch: Birmingham, England, 1974; Vol. IV.

(30) Long, G. J.; Whitney, D. L.; Kennedy, J. E. *Inorg. Chem.* **1971**, *10*, 1406.

(31) Sander, M.; Burmeister, D. *Chem. Ber.* **1962**, *95*, 964.

(32) *Organic Syntheses*; Wiley: New York, 1973; Collect. Vol. V, p 736.

Table X. Elemental Analyses of Cobalt(II) Complexes

			% calcd				% found			
	R^1		C	H	N	M	C	H	N	M
VIa	$(CH_2)_5$	$C_{24}H_{40}N_6Co(PF_6)_2$	37.85	5.29	11.04	7.71	38.03	5.38	11.45	7.54
VIb	$(CH_2)_6$	$C_{25}H_{42}N_6Co(PF_6)_2{\cdot}H_2O$	37.84	5.59	10.59		37.12	5.56	10.30	
VIc	$(CH_2)_7$	$C_{26}H_{44}N_6Co(PF_6)_2$	39.55	5.61	10.64		39.48	5.62	10.62	
VId	$(CH_2)_8$	$C_{27}H_{46}N_6Co(PF_6)_2$	40.35	5.77	10.45		41.32	6.03	10.72	
VIe	$(CH_2)_{12}$	$C_{31}H_{54}N_6Co(PF_6)_2$	43.30	6.33	9.77		43.58	6.39	9.82	
VIf	*m*-xylylene	$C_{27}H_{38}N_6Co(PF_6)_2$	40.76	4.81	10.56		40.53	4.89	10.31	

pound was further purified by chromatography on CM Sephadex eluted with 0.2 M Na_2SO_4. Yield: 8%.

(2,3,10,11,13,19-Hexamethyl-3,10,14,18,21,24-hexaazabicyclo[10.7.6]pentacosa-1,11,13,18,20,24-hexaene-κ⁴*N*)nickel(II) Hexafluorophosphate (Vb, $R^1 = (CH_2)_6$, $R^2 = R^3 = CH_3$). This complex was prepared as reported previously.[12]

(2,3,11,12,14,20-Hexamethyl-3,11,15,19,22,25-hexaazabicyclo[11.7.6]hexacosa-1,12,14,19,21,25-hexaene-κ⁴*N*)nickel(II) Hexafluorophosphate (Vc, $R^1 = (CH_2)_7$, $R^2 = R^3 = CH_3$). Yield: 20%. Anal. Calcd for $C_{26}H_{44}N_6NiP_2F_{12}$: C, 39.56; H, 5.61. Found: C, 39.99; H, 5.80.

(2,3,12,13,15,21-Hexamethyl-3,12,16,20,23,26-hexaazabicyclo[12.7.6]heptacosa-1,13,15,20,22,26-hexaene-κ⁴*N*)nickel(II) Hexafluorophosphate (Vd, $R^1 = (CH_2)_8$, $R^2 = R^3 = CH_3$). Yield: 7%. Anal. Calcd for $C_{27}H_{46}N_6NiP_2F_{12}$: C, 40.36; H, 5.77. Found: C, 40.86; H, 5.92.

(2,3,16,17,19,25-Hexamethyl-3,16,20,24,27,30-hexaazabicyclo[16.7.6]hentriaconta-1,17,19,24,26,30-hexaene-κ⁴*N*)nickel(II) Hexafluorophosphate (Ve, $R^1 = (CH_2)_{12}$, $R^2 = R^3 = CH_3$). Yield: 4%. Anal. Calcd for $C_{31}H_{54}N_6NiP_2F_{12}$: C, 43.31; H, 6.33; N, 9.78. Found: C, 43.54; H, 6.54; N, 9.78.

(2,3,11,12,14,20-Hexamethyl-3,11,15,19,22,25-hexaazatricyclo[11.7.6.1^{5,9}]heptacosa-1,5,7,9(27),12,14,19,21,25-nonaene-κ⁴*N*)nickel(II) Hexafluorophosphate (Vf, R^1 = *m*-Xylylene, $R^2 = R^3 = CH_3$). Yield: monomer, 15%; dimer, 20%. Anal. Calcd for $C_{27}H_{38}N_6NiP_2F_{12}$: C, 40.77; H, 4.81; N, 10.57. Found: C, 4.64; H, 4.90; N, 10.49.

(2,10,12,18-Tetramethyl-3,9,13,17,20,23-hexaazabicyclo[9.7.6]tetracosa-1,10,12,17,19,23-hexaene-κ⁴*N*)nickel(II) Hexafluorophosphate (Vg, $R^1 = (CH_2)_5$, R^2 = H, $R^3 = CH_3$). Yield: monomer, 6%; dimer, 30%. Anal. Calcd for dimer $C_{44}H_{72}N_6NiP_2F_{12}$: C, 36.03; H, 4.94; N, 11.46. Found: C, 36.14; H, 5.03; N, 11.46.

(2,12,14,20-Tetramethyl-3,11,15,19,22,25-hexaazatricyclo[11.7.6.1^{5,9}]heptacosa-1,5,7,9(27),12,14,19,21,25-nonaene-κ⁴*N*)nickel(II) Hexafluorophosphate (Vh, R^1 = *m*-Xylylene, R^2 = H, $R^3 = CH_3$). Yield: monomer, 10%; dimer, 2%.

Preparation of the Ligand Salts. The ligand salts were prepared in a manner similar to that reported for the 16-membered-ring derivatives.[12] HCl(g) was bubbled through a solution of the nickel cyclidene complex in acetonitrile (20 mL) until a blue-green color was obtained (or for a maximum of 5 min). If no color change occurred, the solution was allowed to stand until a significant color change occurred (1.5 h for R^1 = *m*-xylylene). The ligand was precipitated as the $ZnCl_4^{2-}$ salt and was metathesized to the PF_6^- salt. Yields of the ligand salts obtained are tabulated in Table IX.

Synthesis of Cobalt Complexes. The method of synthesis is essentially the same for all of the cobalt complexes. The procedure is given for VIa.

(2,3,9,10,12,18-Hexamethyl-3,9,13,17,20,23-hexaazabicyclo[9.7.6]-tetracosa-1,10,12,17,19,23-hexaene-κ⁴*N*)cobalt(II) Hexafluorophosphate (VIa, $R^1 = (CH_2)_5$, $R^2 = R^3 = CH_3$). The ligand salt (0.1 g, 0.11 mmol), cobalt acetate tetrahydrate (0.05 g, 0.20 mmol), and sodium acetate trihydrate (0.1 g, 0.73 mmol) were placed in a 50-mL Erlenmeyer flask in a controlled-atmosphere box. Methanol, 20 mL, was added, and the solution was stirred overnight. The bright orange powder was collected by filtration. Yield: 0.05 g, 58%. The analyses for these complexes are listed in Table X.

Synthesis of the Iron(II) Complex. Chloro(2,3,11,12,14,20-hexamethyl-3,11,15,19,22,25-hexaazatricyclo[11.7.6.1^{5,9}]heptacosa-1,5,7,9-(27),12,14,19,21,25-nonaene-κ⁴*N*)iron(II) Hexafluorophosphate Hydrate (VII, R^1 = *m*-Xylylene, $R^2 = R^3 = CH^3$). The free-ligand salt (0.05 g, 0.05 mmol) was dissolved in 5 mL of CH_3CN. A solution of $Fe(py)_2Cl_2$ (0.025 g, 0.088 mmol) in 5 mL of CH_3CN was added. Triethylamine (1 mL, 7.17 mmol) was added, producing a dark red solution. The solvent was removed in vacuo, and methanol (2 mL) was added to dissolve the residue. Upon standing 10 min, the solution yielded dark red solids. These solids were collected by filtration; yield 0.04 g, ~100%. Anal. Calcd for $C_{27}H_{38}N_6FeClPF_6{\cdot}H_2O$: C, 46.28; N, 11.99; H, 5.71; Fe, 7.97. Found: C, 46.41; N, 12.12; H, 5.59; Fe, 7.95.

Solutions for K_{O_2} Measurements. Solutions of the cobalt complexes were prepared in 1.5 M *N*-MIM in CH_3CN at concentrations that produced spectrophotometer absorbance readings of 1.5–2.0 at 380 nm. The spectral changes accompanying changes in O_2 pressure were recorded at 420, 440, and 460 nm. The spectra showed isosbestic points at 390 and 530 nm, indicating that only two detectable absorbing species are present. The procedure for the determination and calculation of the equilibrium constants for O_2 binding was as described previously.[8a,27] For the cobalt complex having $R^1 = (CH_2)_{12}$, $R^2 = R^3 = CH_3$, decomposition occurred when pure dioxygen was bubbled through the solution. The spectra remained isosbestic for dioxygen pressures up to 38 Torr at 20 °C.

Acknowledgment. We wish to thank the National Science Foundation for supporting this research.

Registry No. I($R^1 = (CH_2)_7$, $R^2 = R^3 = CH_3$, M = Co, X = $(CH_2)_3)^{2+}{\cdot}$*N*-MIM, 114534-88-2; I($R^1 = (CH_2)_7$, $R^2 = R^3 = CH_3$, M = Co, X = $(CH_2)_3)^{2+}{\cdot}O_2{\cdot}$*N*-MIM, 114550-36-6; I($R^1 = (CH_2)_8$, $R^2 = R^3 = CH_3$, M = Co, X = $(CH_2)_3)^{2+}{\cdot}$*N*-MIM, 114534-89-3; I($R^1 = (CH_2)_8$, $R^2 = R^3 = CH_3$, M = Co, X = $(CH_2)_3)^{2+}{\cdot}O_2{\cdot}$*N*-MIM, 114550-37-7; IV, 74465-83-1; IV ligand, 114534-96-2; Va, 114534-56-4; Va ligand PF_6 salt, 114534-99-5; Vb, 76791-43-0; Vb ligand PF_6^- salt, 114535-00-1; Vc, 114534-58-6; Vc ligand PF_6^- salt, 114535-02-3; Vd, 114550-29-7; Vd ligand PF_6^- salt, 114535-04-5; Ve, 114534-59-7; Ve ligand PF_6^- salt, 114535-06-7; Vf, 114534-61-1; Vf ligand PF_6^- salt, 114535-08-9; $Vf^{3+}{\cdot}$*N*-MIM, 114534-77-9; Vf dimer, 114534-91-7; Vg, 114534-63-3; $Vg^{3+}{\cdot}$*N*-MIM, 114534-78-0; Vg dimer, 114534-93-9; Vh, 114534-65-5; $Vh^{3+}{\cdot}$*N*-MIM, 114534-79-1; Vh dimer, 114534-95-1; VIa, 114534-67-7; $VIa^{2+}{\cdot}$*N*-MIM, 114534-87-1; $VIa^{2+}{\cdot}O_2{\cdot}$*N*-MIM, 114550-35-5; $Vf^{2+}{\cdot}$*N*-MIM, 114614-05-0; VIb, 114534-68-8; $VIb^{2+}{\cdot}$*N*-MIM, 114534-82-6; $VIb^{2+}{\cdot}O_2{\cdot}$*N*-MIM, 114550-30-0; VIc, 114534-69-9; $VIc^{2+}{\cdot}$*N*-MIM, 114534-83-7; $VIc^{2+}{\cdot}O_2{\cdot}$*N*-MIM, 114550-31-1; VId, 114534-70-2; $VId^{2+}{\cdot}$*N*-MIM, 114534-84-8; $VId^{2+}{\cdot}O_2{\cdot}$*N*-MIM, 114550-32-2; VIe, 114534-72-4; $VIe^{3+}{\cdot}CH_3CN$, 114534-80-4; $VIe^{2+}{\cdot}$*N*-MIM, 114534-85-9; $VIe^{2+}{\cdot}O_2{\cdot}$*N*-MIM, 114550-33-3; VIf, 114534-74-6; $VIf^{3+}{\cdot}CH_3CN$, 114534-81-5; $VIf^{2+}{\cdot}$*N*-MIM, 114534-86-0; $VIf^{2+}{\cdot}O_2{\cdot}$*N*-MIM, 114550-34-4; VII, 114534-76-8; $CH_3NH(CH_2)_5NHCH_3$, 56992-95-1; $CH_3NH(CH_2)_6NHCH_3$, 13093-04-4; $CH_3NH(CH_2)_7NHCH_3$, 15411-11-7; $CH_3NH(CH_2)_8NHCH_3$, 33563-54-1; $CH_3NH(CH_2)_{12}NHCH_3$, 56992-91-7; CH_3NHCH_2-*m*-$C_6H_4CH_2NHCH_3$, 114534-97-3; $H_2N(CH_2)_5NH_2$, 462-94-2; H_2NCH_2-*m*-$C_6H_4CH_2NH_2$, 1477-55-0; C_6H_5CHO, 100-52-7; $H_2N(CH_2)_6NH_2$, 124-09-4; $H_2N(CH_2)_7NH_2$, 646-19-5; $H_2N(CH_2)_8NH_2$, 373-44-4; $H_2N(CH_2)_{12}NH_2$, 2783-17-7; $Fe(py)_2Cl_2$, 15616-26-9; dimethyl sulfate, 77-78-1; $Vg^{2+}{\cdot}$*N*-MIM, 114614-06-1; $Vh^{2+}{\cdot}$*N*-MIM, 114614-07-2.

Supplementary Material Available: Tables S2–S5, listing remaining bond lengths, remaining bond angles, temperature factors, and hydrogen positions for Vb, and Figure S1, showing a packing diagram for Vb (4 pages); Table S1, listing observed and calculated structure factors (30 pages). Ordering information is given on any current masthead page.